Center for Turbulence Research
Proceedings of the Summer Program 2010

Modeling roughness effects in turbulent boundary layers by elliptic relaxation

By J. George†, A. De Simone, G. Iaccarino AND J. Jiménez‡

The modeling of roughness effects in turbulent boundary layers (TBLs) is considered using the elliptic relaxation method of Durbin (1993), which takes into account non-local, wall-blocking effects. His approach considers a term, analogous to energy redistribution, that combines the effects of the near-wall velocity-pressure gradient correlation and the anisotropic dissipation rate and, by extension, the near-wall stress anisotropy and the non-local pressure-strain effects. An extensive experimental data-set comprising smooth-wall and various rough-wall TBLs over distributed three-dimensional roughness (George 2005) is used to quantify this term and its response to roughness. Further, this data-set is used to estimate appropriate length and time scales for rough-wall, which are used to modify the elliptic relaxation in the $\overline{v^2} - f$ model framework. A priori testing of eddy viscosity using the data confirms that wall-normal stress ($\overline{v^2}$) is a more appropriate velocity scale than turbulence kinetic energy in rough-wall computations.

1. Introduction

The calculation of roughness effects on wall-bounded flows poses major challenges so much that V.C. Patel entitled his lecture, Flow at High Reynolds Number and Over Rough Surfaces-Achilles Heel of CFD (Patel 1998), a statement that still holds good. Recent studies on computation of rough-wall flows have used Direct Numerical Simulation (DNS) and Large Eddy Simulations (LES), but the resolution requirements needed to resolve the roughness geometry, especially those involving three-dimensional roughness, and the need to resolve a hierarchy of scales from the smallest scales to the outer length scales make the solutions impractical for high-Reynolds number flows. Hence it is necessary need to develop and use robust Reynolds-averaged Navier-Stokes (RANS) models for applications to complex flows and geometries such as the rough-wall flows.

Among RANS models, Durbin's $\overline{v^2} - f$ model (Durbin 1993) is particularly attractive owing to its relatively simple formulation. It is a better alternative to the conventional $k - \epsilon$ model because the $\overline{v^2} - f$ model is suitable right up to the wall and does not need damping functions to mimic the attenuation of turbulence close to the wall in the case of smooth-walls. For rough-walls, the low-Reynolds-number $k - \epsilon$ models need damping functions that include equivalent sand grain roughness in order to obtain the effect of increased turbulent mixing near the rough-wall (Lu & Liou 2007). The need for damping functions is avoided in the $\overline{v^2} - f$ model by incorporating near-wall turbulence anisotropy and non-local pressure-strain effects through an elliptic relaxation equation that captures the non-local, wall-blocking effects. This feature is crucial not only in the computation of strongly heterogeneous flows such as rough-wall flows but also toward accurate prediction of heat transfer, skin friction, and turbulent boundary layer separation.

Some examples of complex flows computed satisfactorily using the $\overline{v^2} - f$ model are

† Innovative Aerospace Solutions, Downey, CA
‡ Also, School of Aeronautics, Universidad Politécnica de Madrid, Spain

subsonic and transonic flow around airfoils (Kalitzin 1999), flows with adverse pressure gradient and around bluff bodies (Durbin 1995), and three-dimensional pressure-driven turbulent boundary layers around a wing-body junction (Parneix *et al.* 1998). The main features of the mean quantities and the turbulence kinetic energy (k) were adequately reproduced despite the fact that the model employed linear eddy viscosity hypothesis. The attraction of fewer equations and more robustness than Reynolds stress models, along with inclusion of elliptical relaxation in a linear eddy viscosity framework, has made the $\overline{v^2} - f$ model quite popular, and it is now also available in several commercial codes (Iaccarino, 2001, Gatski *et al.* 2007).

With the above mentioned reasons, there is more than sufficient impetus to model roughness effects using the $\overline{v^2} - f$ model. This would be quite different from most of the engineering RANS models that have been developed for rough-walls where the modifications to the log-law are directly incorporated through an ad-hoc tuning of the model coefficients. To the authors' best knowledge, this is the first time the $\overline{v^2} - f$ model is used in the computation of rough-wall flows over distributions of three-dimensional roughness, and hence it is very important to study the behavior of this turbulence model to roughness effects.

In the $\overline{v^2} - f$ model (Durbin & Pettersson Reif 2001), the system of equations for the Reynolds stress tensor (τ_{ij}) is replaced by a transport equation for a velocity scalar, $\overline{v^2}$, and an elliptic equation is introduced for a function, f, which is analogous to an energy redistribution term. This term represents the combined effects of near-wall velocity-pressure-gradient correlation and the anisotropic dissipation rate. One goal of the present investigation is to look at the possibility that modifications to this energy redistribution can be correlated to the roughness. This is made possible by examining the experimental data of George (2005) wherein the flow structure within and above a rough surface in moderately high-Reynolds number turbulent-boundary layers (TBL) was explored in great detail with a three-orthogonal-velocity-component Laser Doppler Velocimeter. Different surfaces containing sparse distribution of cylinders, with heights (h) to boundary layer thickness (δ) ratios of less than 2.5%, generate fully developed flows that range from transitionally rough to fully rough. The full complement of mean velocities, Reynolds stresses and triple products are used to estimate the term analogous to the energy redistribution term. The second goal of this study is to obtain turbulence length and time scales from the experimental study for their use in the computations of rough-wall flows using the $\overline{v^2} - f$ model.

2. Approach

2.1. *Details of the experiments*

Detailed 3-orthogonal-velocity-component Laser-Doppler Velocimetry (LDV) and other measurements were performed to understand and describe the rough-wall flow structure (George 2005). The measurements include mean velocities, turbulence quantities (Reynolds stresses and triple products), surface pressure, and oil flow visualizations in fully developed two-dimensional rough-wall flows for Reynolds numbers (Re_θ), based on momentum thickness (θ), ranging from 7000 to 15000. Uniform circular cylindrical roughness elements of 0.38, 0.76 and 1.52 mm height (h) were used in square and staggered patterns, yielding six different roughness geometries of rough-wall surface. The roughness Reynolds numbers (h^+) based on the element height (h) and the friction velocity (U_τ), range from 26 to 131. A detailed grid of profiles (40-45) was measured within the

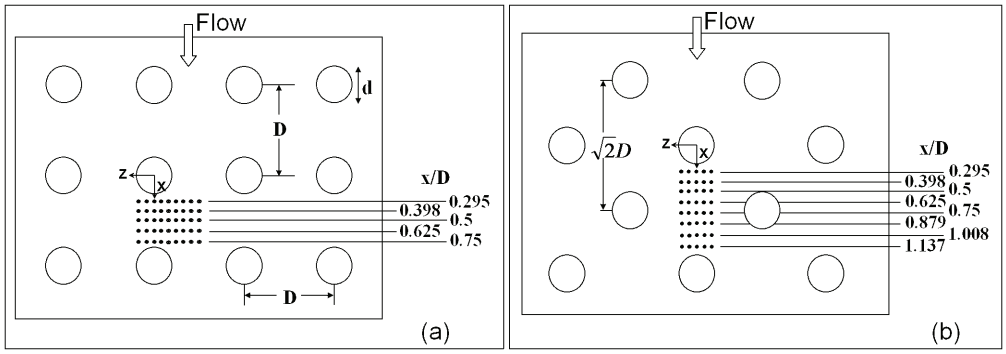

FIGURE 1. Measurement locations in the two-dimensional rough-wall boundary layers: (a) straight orientation, (b) staggered orientation. Each point represents a profile in the wall-normal direction. The cylinder diameter (d) is 1.98 mm, and center-to-center spacing (D) is 5.49 mm.

Case	h (mm)	Orientation	U_e (m/s)	δ (mm)	δ^* (mm)	θ (mm)	Re_θ	h/δ	U_τ (m/s)	h^+
0	0	smooth wall	26.97	39.0	6.09	4.47	7300	-	0.966	-
1	0.38	straight	27.19	51.9	8.68	5.92	9179	0.0073	1.131	26
2	0.38	staggered	27.34	51.2	8.72	6.02	9945	0.0074	1.144	26
3	0.76	straight	27.56	58.5	11.28	7.25	12067	0.013	1.272	59
4	0.76	staggered	27.37	58.7	11.38	7.40	12231	0.013	1.295	60
5	1.52	straight	27.51	63.1	13.94	8.30	13789	0.024	1.394	128
6	1.52	staggered	27.20	70.4	14.77	9.03	14828	0.022	1.420	131

TABLE 1. Boundary layer parameters for the smooth wall and the six cases of two-dimensional rough-wall turbulent boundary layers at $x/D = 0.5$, $z/d = 0$. Kinematic viscosity $\nu = 1.656\times\ 10^{-5}\ m^2/s$.

rough-wall and around the roughness elements, as shown in Fig. 1. These measurements are used to obtain the various terms in the transport-rate equations for the wall-normal Reynolds stresses ($\overline{v^2}$) and turbulence kinetic energy (k). Table 1 presents a summary of the flow cases along with their boundary layer parameters.

2.2. *Details of the modeling approach*

For incompressible flows, the Reynolds stress transport equations can be written as

$$\frac{\partial \overline{u_i u_j}}{\partial t} + C_{ij} = P_{ij} + \Pi_{ij} - \epsilon_{ij} + TD_{ij} + VD_{ij} \tag{2.1}$$

where,

$$\text{Convection: } C_{ij} = U_k \frac{\partial \overline{u_i u_j}}{\partial x_k}, \tag{2.2}$$

$$\text{Production: } P_{ij} = -\overline{u_j u_k}\frac{\partial U_i}{\partial x_k} - \overline{u_i u_k}\frac{\partial U_j}{\partial x_k}, \tag{2.3}$$

$$\text{Velocity-pressure gradient correlation: } \Pi_{ij} = -\overline{u_i \frac{\partial p}{\partial x_j}} - \overline{u_j \frac{\partial p}{\partial x_i}}, \tag{2.4}$$

$$\text{Dissipation: } \epsilon_{ij} = 2\nu\overline{\frac{\partial u_i}{\partial x_k}\frac{\partial u_j}{\partial x_k}}, \tag{2.5}$$

$$\text{Turbulent diffusion: } TD_{ij} = -\frac{\partial\overline{u_i u_j u_k}}{\partial x_k}, \tag{2.6}$$

$$\text{Viscous diffusion: } VD_{ij} = \nu\frac{\partial^2\overline{u_i u_j}}{\partial x_k \partial x_k}. \tag{2.7}$$

Following Durbin (1993) we can recast equation (2.1) as

$$\frac{\partial\overline{u_i u_j}}{\partial t} + C_{ij} + \epsilon\frac{\overline{u_i u_j}}{k} = P_{ij} + \underbrace{\Pi_{ij} - \left(\epsilon_{ij} - \epsilon\frac{\overline{u_i u_j}}{k}\right)}_{\phi_{ij}=kf_{ij}} + TD_{ij} + VD_{ij}, \tag{2.8}$$

where k is the turbulence kinetic energy and ϵ its dissipation rate. The relaxation tensor function (f_{ij}) is determined by the following elliptic PDE:

$$L^2\frac{\partial^2 f_{ij}}{\partial x_k \partial x_k} - f_{ij} = -\frac{\phi_{ij}^{qh}}{k} - \frac{b_{ij}}{T}, \tag{2.9}$$

where L and T are the appropriate turbulence length and time scales, and b_{ij} is the anisotropy tensor, defined as

$$b_{ij} \equiv \frac{\overline{u_i u_j}}{k} - \frac{2}{3}\delta_{ij}. \tag{2.10}$$

Considering the $\overline{v^2} - f$ system, Eqs. (2.7) and (2.8) reduce to

$$\frac{\partial\overline{v^2}}{\partial t} + U_j\frac{\partial\overline{v^2}}{\partial x_j} + \epsilon\frac{\overline{v^2}}{k} = P_{vv} + kf - \frac{\partial\overline{v^2 u_j}}{\partial x_j} + \nu\frac{\partial^2\overline{v^2}}{\partial x_j \partial x_j}, \tag{2.11}$$

$$L^2\nabla^2 f - f = -\frac{\phi^{qh}}{k} - \frac{b_{22}}{T}, \tag{2.12}$$

where $\phi = kf$, $T = k/\epsilon$, and $b_{22} \equiv (\overline{v^2}/k - 2/3)$. The present study uses the Rotta+IP (isotropization of production) model as the source term, ϕ^{qh} (Manceau & Hanjalic, 2000). The basic premise behind roughness modeling is to introduce modified length and time scales in the elliptic PDE in order to modify the damping due to the roughness.

2.3. *Determination of the analogous term to the energy redistribution (ϕ) and the relaxation function (f)*

As seen from Eq. (2.8), ϕ is the sum of velocity-pressure gradient correlation and the anisotropic dissipation and is equal to kf in Eq. (2.11). This term can be obtained as a remainder because all the other terms can be calculated using the experimental data-set of George (2005). The dissipation of k (ϵ) is obtained as a remainder of the k budget if the pressure-diffusion term can be modeled (Lumley 1978) because all the other terms can be calculated. Note that owing to continuity, the pressure-strain term in k budget goes to zero.

2.4. *The $\overline{v^2} - f$ model equations*

The following equations are in addition to the system of equations for the $k-\epsilon$ model (see Appendix B, Manceau & Hanjalic, 2000). The equation for $\overline{v^2}$ is obtained by ignoring its production term in Eq. (2.11) and the turbulent diffusion is modeled using a gradient approach.

$$\frac{D\overline{v^2}}{Dt} = kf - \epsilon\frac{\overline{v^2}}{k} + \nabla\cdot\left[(\nu+\nu_T)\nabla\overline{v^2}\right], \tag{2.13}$$

$$L^2\nabla^2 f - f = (1-C_1)\frac{(2/3-\overline{v^2}/k)}{T} - C_2\frac{P}{k}. \tag{2.14}$$

The eddy viscosity $\nu_T = C_\mu\overline{v^2}T$, and $P = 2\nu_T S_{ij}S_{ij}$, where $S_{ij} = 1/2(\frac{\partial U_i}{\partial x_j} + \frac{\partial U_j}{\partial x_i})$. The length ($L$) and time ($T$) scales of turbulence are defined by

$$L = C_L max\left[\frac{k^{3/2}}{\epsilon}, C_\eta\left(\frac{\nu^3}{\epsilon}\right)^{1/4}\right], \tag{2.15}$$

$$T = max\left[\frac{k}{\epsilon}, C_T\left(\frac{\nu}{\epsilon}\right)^{1/2}\right]. \tag{2.16}$$

The bound is to ensure that the scales are above the Kolmogorov scales. The model constants are $C_\mu = 0.22$, $C_1 = 1.22$, $C_2 = 0.6$, $C_T = 6.0$, $C_L = 0.2$, $C_\eta = 80.0$. The wall boundary conditions are: $U_i = 0$, $k = 0$, $\overline{v^2} = 0$, $\epsilon = 2\nu k/y^2$, $f = -20\nu^2\overline{v^2}/(\epsilon y^4)$.

3. Results and discussion

It should be noted that the results presented here are those obtained by averaging over a plane at a constant distance from the wall, and hence they are not location-dependent within the rough-wall.

Figure 2 shows the distributions of the term analogous to energy redistribution, ϕ^+, for various rough-wall cases, where $\phi^+ = \phi/(U_\tau^4/\nu)$. For the sake of comparison, the plot also displays those for smooth-wall channels and TBLs obtained using DNS. Although the smooth-wall TBLs show similar behavior in their distributions, those for the rough-wall are starkly different. For a smooth-wall, the distributions display gentle peaks at about y^+ of 35, just above the buffer layer, which is considerably farther away from the location of y^+ of 10-15 where peak production of k occurs. The latter location is also close to the region denoting peak dissipation of k. Perhaps the behavior of the maxima of ϕ distributions is related to the diffusion of turbulence and its redistribution through pressure fluctuations to regions away from these peak locations. For the rough-walls, however, the peaks of both production of k and its dissipation, also production of $\overline{v^2}$ stress (which is primarily due to the term $\overline{v^2}\partial V/\partial y$), occur in the neighborhood of the element height, and large levels of turbulence are transported and redistributed from these regions throughout the roughness sublayer region that extend to three element heights (George 2005). This behavior perhaps explains the location of peaks in the distributions of ϕ^+ at regions slightly above the element height.

The distributions of ϕ^+, when plotted as an offset with the roughness height (h^+) in Fig. 3, indicate that the width of the ϕ^+ distribution is related to the diameter of the roughness element. Also, the peak values of the distribution, ϕ^+_{max}, display an exponential decay with roughness height as seen in Fig. 4. The behavior of the elliptic relaxation function, f^+, which is ϕ^+/k, is similar to those for the ϕ^+ distribution but is not shown here for the sake of brevity.

The length (L) and time (T) scales resulting from flow turbulence, used in the $\overline{v^2} - f$

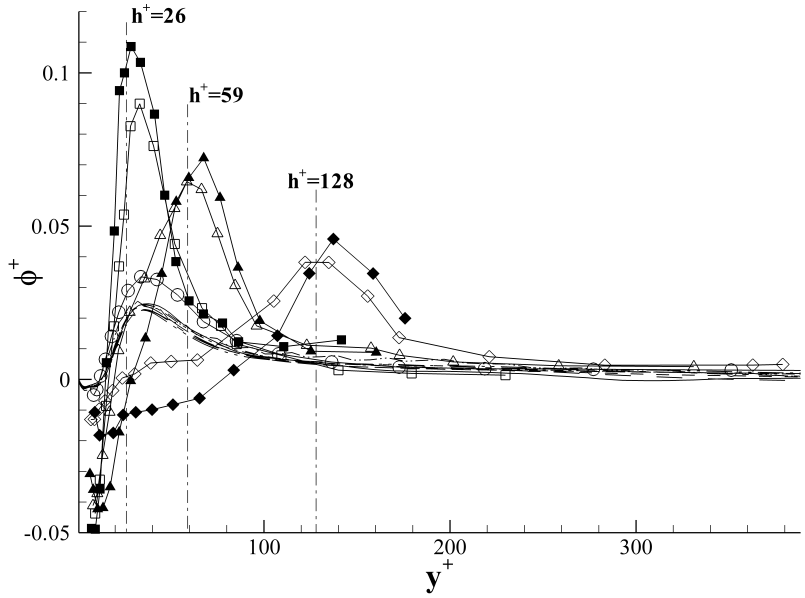

FIGURE 2. Variation of the term analogous to energy redistribution (ϕ^+) with distance from the wall (y^+). The dashed lines indicate the location of the roughness element height. —— $Re_\tau = 395$ (Kim et al. 1987); – – – $Re_\tau = 590$ (Moser et al. 1999); – - – $Re_\tau = 950$ (Del Alamo et al. 2004); — — $Re_\tau = 2000$ (Jiménez et al. 2010); .. - .. - $Re_\theta = 1410$ (Spalart 1988); — — $Re_\theta = 1100$ (Jiménez et al, 2010); — . — $Re_\theta = 1551$ (Jiménez et al. 2010) ; — . . —$Re_\theta = 1968$ (Jiménez et al. 2010) ; ∘ $Re_\theta = 7300$ (George 2005) ; ▫ Rough-wall, h =0.38 mm; △ Rough-wall, $h = 0.76\ mm$; ⋄ Rough-wall, $h = 1.52\ mm$; straight orientation: open symbols; staggered orientation: closed symbols.

model, are given by $L = C_L(k^{3/2}/\epsilon)$, and $T = k/\epsilon$ (Eqs. 2.15 and 2.16). The nondimensionalized length scale, $L^+ = LU_\tau/\nu$, and time scale, $T^+ = TU_\tau^2/\nu$, are plotted as a variation with distance from the wall in Fig. 5. The results reveal that the variation is fairly constant within the rough-wall, up to the roughness element height, which is indicative of the low-momentum separated flow regions within the rough-wall. The constancy in the length scale behavior is also similar to that outlined for mixing length in the canopy model for three-dimensional roughness elements (Belcher *et al.* 2003). The length scales are of the order of the roughness height and are representative of the eddies formed behind the roughness elements. Further, both constant length (L_h^+) and time (T_h^+) scales vary almost linearly with increase in the element height, as shown in Fig. 6, and these constant scales are used in the elliptic relaxation Eqs. (2.12 and 2.14) to provide the appropriate modification caused by roughness.

A priori testing of eddy viscosity from the experimental data using the $\overline{v^2} - f$ model equations indicates that eddy viscosity can be satisfactorily reproduced as shown in Fig. 7, where nondimensionalized eddy viscosity, $\nu_T^+ = \nu_T/\nu$, is presented as a variation with distance from the wall. The closed symbols indicate actual eddy viscosity obtained from the data, which is $-\overline{uv}/(\partial U/\partial y)$, and open symbols indicate those obtained using the model equation, $\nu_T = C_\mu \overline{v^2} T$, where T is the time scale. The satisfactory agreement also demonstrates that $\overline{v^2}$ is the more appropriate velocity scale rather than turbulence

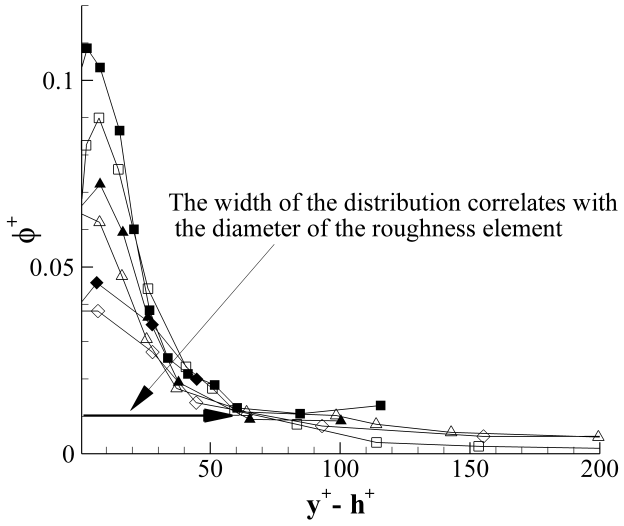

FIGURE 3. Variation of ϕ^+, with distance from the wall (y^+) offset by nondimensionalized element height, h^+. ◘ Rough-wall, h =0.38 mm; △ rough-wall, h = 0.76 mm; ◇ rough-wall, $h = 1.52$ mm; straight orientation: open symbols; staggered orientation: closed symbols.

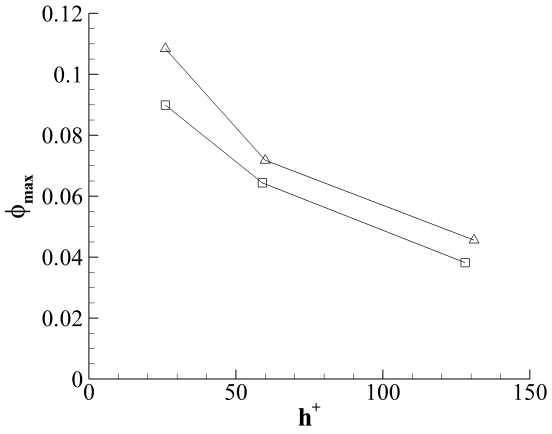

FIGURE 4. Variation of ϕ^+_{max} with nondimensionalized element height, h^+. Two-dimensional rough-wall TBL, straight: ◘ ; two-dimensional rough-wall TBL, staggered: △.

kinetic energy (k). For the sake of brevity, plots obtained using the latter as a velocity scale are not shown here.

4. Conclusions

A modeling scheme is outlined to compute rough-wall turbulent boundary layers using the elliptic relaxation scheme within the $\overline{v^2} - f$ model framework. The data-sets obtained from the LDV measurements of various transitionally rough and fully rough two-dimensional turbulent boundary layers are used to obtain the various terms in the

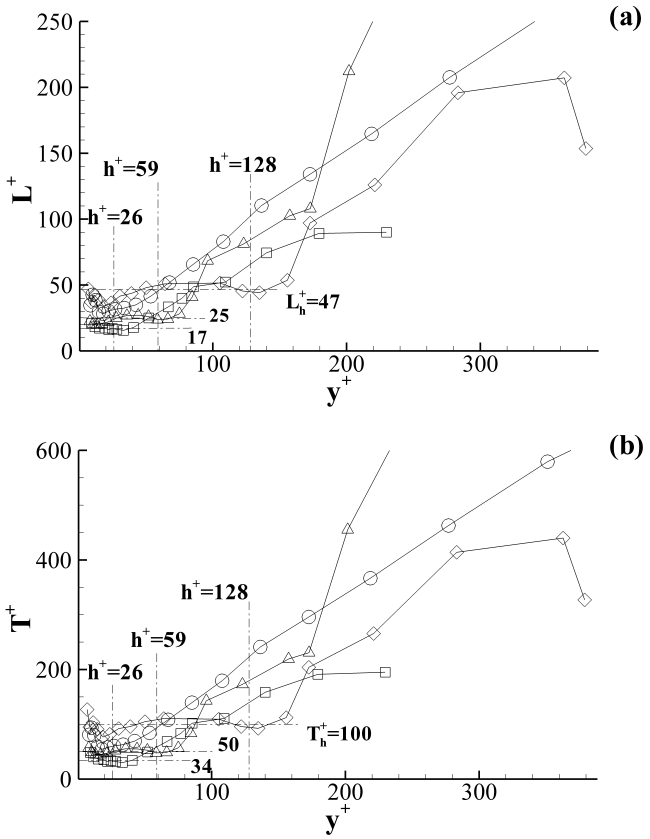

FIGURE 5. Variation of roughness scales with distance from the wall, y^+. (a) Length scale, L^+; (b) Time scale, T^+. The dashed lines parallel to the x-axis denote the constancy in the value of the scales along with their values. Smooth-wall, Re_θ=7300 (George, 2005): ○; Rough-wall, straight, h =0.38 mm: □ ; Rough-wall, straight, h =0.76 mm: △; Rough-wall, straight, h =1.52 mm: ◇.

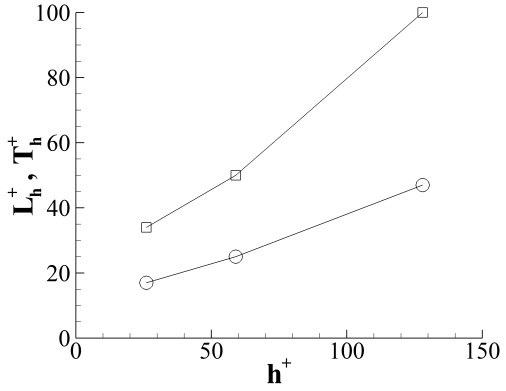

FIGURE 6. Variation of constant roughness length and time scales with nondimensionalized element height, h^+. Length scale L_h^+: ○; time scale T_h^+: □

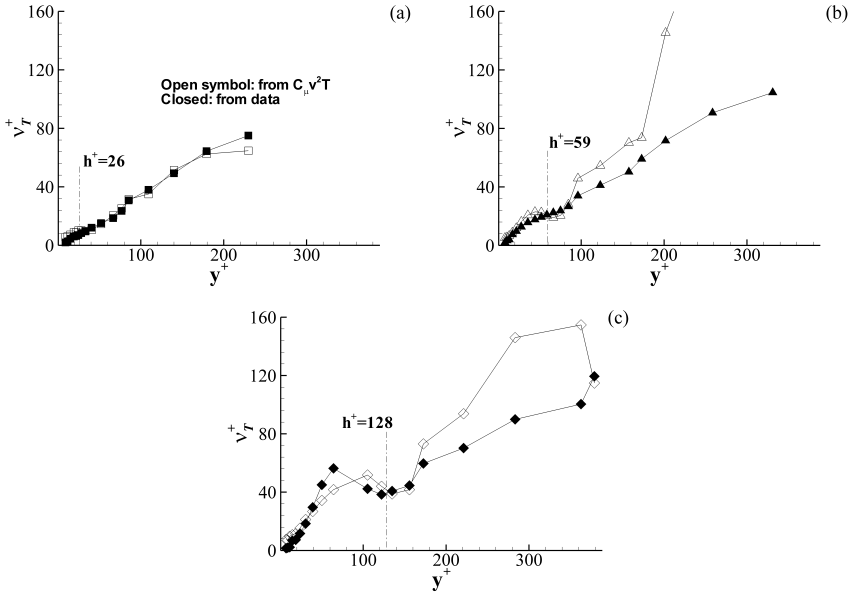

FIGURE 7. Comparison of eddy viscosity, ν_T^+, obtained from the rough-wall experiments with those obtained using the $\overline{v^2} - f$ model equations: (a) h =0.38 mm, straight: ▫ (b) h =0.76 mm, straight: △; (c) h =1.52 mm, straight: ◇. From $C_\mu \overline{v^2} T$: open symbols; from data: closed symbols.

budgets of wall-normal stress ($\overline{v^2}$) and turbulence kinetic energy (k). The analysis reveals that the variations in the term analogous to the energy redistribution term, ϕ, is related to the dimensions of the roughness element, and further, their maxima and that for the elliptic relaxation function, f, occur close to the element height. Also, their peak values decay exponentially with increase in the element height. The variations of length scales and time scales in the rough-wall reveal that they are constant within the rough-wall, and these constant values increase almost linearly with increase in the element height. The roughness effects are incorporated through the use of these constant scales which are used to modify the elliptic relaxation equation in the $\overline{v^2} - f$ model. A priori testing of eddy viscosity obtained from the experiments reveal that the $\overline{v^2} - f$ model is able to satisfactorily calculate the eddy viscosities using the velocity scale, $\overline{v^2}$, and the time scale from rough-wall flows. Furthermore, $\overline{v^2}$ is a more appropriate velocity scale than k.

5. Acknowledgements

The first author gratefully acknowledges the Office of Naval Research (ONR) for support for the experiments performed during his Doctoral studies at Virginia Tech. He is very thankful to CTR, Stanford for the summer fellowship.

REFERENCES

BELCHER, S.E., JERRAM, N. & HUNT, J.C.R. 2003 Adjustment of a turbulent boundary layer to a canopy of roughness elements. *J. Fluid Mech.*, 488, 369-398.

DEL ALAMO, J.C., JIMÉNEZ, J., ZANDONADE, P. & MOSER, R.D. 2004 Scaling of the energy spectra of turbulent channels. *J. Fluid Mech.*, 500, 135-144.

Durbin, P.A. 1993 A Reynolds stress model for near-wall turbulence. *J. Fluid Mech.*, 249, 465-498.

Durbin, P.A. 1995 Separated flow computations with the $k-\epsilon-\overline{v^2}$ model. *AIAA J.*, 33, 659-664.

Durbin, P.A. & Pettersson Reif, B.A. 2001 *Statistical Theory and Modeling for Turbulent Flows*. Wiley, New York.

Gatski, T.B., Rumsey, C.L. & Manceau, R. 2007 Current trends in modeling research for turbulent aerodynamic flows. *Phil. Trans. R. Soc. A*, 365, 2389-2418.

George, J. 2005 Structure of two-dimensional and three-dimensional turbulent boundary layers with sparsely distributed roughness elements. *Ph.D. Dissertation*, Department of Aerospace and Ocean Engineering, Virginia Polytechnic Institute and State University.

Iaccarino, G. 2001 Predictions of a turbulent separated flow using commercial CFD codes. *J. Fluids Eng.*, 123 (4), 819-828.

Jiménez, J., Hoyas, S., Simens, M.P. & Mizuno, Y. 2010 Turbulent boundary layers and channels at moderate Reynolds numbers. *J. Fluid Mech.*, 657, 335-360.

Kalitzin, G. 1999 Application of the $\overline{v^2}-f$ model to aerospace configurations. Center for Turbulence Research. *Ann. Res. Briefs*.

Kim, J., Moin, P. & Moser, R.D. 1987 Turbulence statistics in fully developed channel flow at low Reynolds number. *J. Fluid Mech.*, 177, 133-166.

Lu, M.H. & Liou, W.W. 2007 Assessment of two low-Reynolds-Number $k-\epsilon$ models in turbulent boundary layers with surface roughness. *J. Spacecraft Rockets,* 44, (6), 1307-1316.

Lumley, J.L. 1978 Computational modeling of turbulent flows. *Adv. Appl. Mech.*, 18, 123- 176.

Manceau, R. & Hanjalic, K. 2000 A new form of the elliptic relaxation equation to account for wall effects in RANS modeling. *Phys. Fluids*, 12 (9), 2345-2351.

Moser, R.D., Kim, J. & Mansour, N.N. 1999 Direct numerical simulation of turbulent channel flow up to $Re_\tau = 590$. *Phys. Fluids*, 11 (4), 943-945.

Parneix, S., Durbin, P.A. & Behnia, M. 1998 Computation of three-dimensional turbulent boundary layers using the $\overline{v^2}-f$ model. *Flow, Turbulence Combust.*, 60, 19-46.

Patel, V.C. 1998 Perspective: flow at high reynolds number and over rough surfaces - Achilles heel of CFD. *J. Fluids Eng.* 120, 434-44.

Spalart, P.R. 1988 Direct simulation of a turbulent boundary layer up to $Re_\theta = 1410$. *J. Fluid Mech.*, 187, 61-98.